Dream Prediction

Nihal Ezgi Yuceturk

January 18, 2019

Abstract

Usage of neural networks in neuroimaging area is becoming increasingly common due to their representation power. Especially ConvNets area particularly popular in the classification of Electroencephalogram (EEG) and Magnetic Resonance Imaging (fMRI). Herein, we worked on modelling and classification of patterns exist in EEG recordings of dreaming brain. We reduced it into image and video classification problem while preserving multimodel information of EEG. Our best spatiotemporal networks display 85% accuracy in distinguishing signals of dreaming brain from not dreaming. We further studied to distinguish recalling ability of dreams. The same networks achieved 55% accuracy. We showed that although more subtle, dreaming as other cognitive events can be detected via EEG classification with neural networks.

Contents

1 INTRODUCTION

Neural networks have recently gained great popularity in feature learning and recognition tasks due to their highly customizable structures for specific tasks and their robustness to variation in data. [1, 2] Particularly, Convolutional Neural Networks made an appearance within a wide range of applications especially in image and video classification tasks whereas Recurrent Neural Networks have shown remarkable performance in dynamic temporal sequences such as handwriting and speech recognition.

Although it seems quite promising, applications of neural networks in neuroimaging domain are relatively new. Perhaps the main reasons are first, the lack of sufficient datasets; that is the number of samples in neuroimaging datasets is limited which makes it harder to train deep networks with millions of parameters. Second, the lack of interpretability; that is to find a direct connection with input features and neural network representations is troublesome. For the latter, hand-designed feature selection techniques have been developed for many years by domain experts and various machine learning techniques have been applied like Filter Bank Common Spatial Patterns (FBCSP) [3]. It is now a benchmark which is already remarkably successful and comprehensible but requires multiple, computationally heavy preprocessing steps.

Here we explored the capacities of neural networks for modelling and classifying perhaps the most mysterious cognitive event *dreaming* from EEG data. EEG decoding and representation learning have been studied recently by using neural networks for mental load classification tasks such as button press or movements of limbs [4, 5, 6] but as far as our knowledge never with such a data where the subject is unconscious. It is known that cognitive task events such as button press creates an obvious, observable (both with EEG and fMRI) and very well defined firing patterns in the brain [5] but until recently, it has not been known such a pattern exists for dreaming stage of the brain. [7] With highly intensive spectral analysis, researches identified that particular regions of the brain are more involved in dreaming experience and recalling it but it is a mystery if those regions can be identified and correlated via neural networks.

Since EEG inherently involves dynamic spatial and temporal patterns it requires careful approaches to make benefit of both patterns. Focusing on temporal features at the cost of sacrificing spatial features, if indeed activation pattern of the cognitive task is very well known, is a successful approach

[4] where each electrode is treated as an independent feature of time series. The aim is then to find a suitable representation of these time series at first and to find a classifier for those representations. Another approach is to threat EEG as an image and to use the power of recent image classification techniques. Temporal patterns might be caught via recurrent architectures after spatial features are extracted as in [5, 6]

We proposed here a mixture of previously studied approaches to classify EEG data as well as a novel approach since we did not know a priori that if the data (EEG recordings of sleeping subjects) can be classified or not via neural networks and if so, how. We barely preprocessed the data except for necessary normalizations to assess end-to-end recognition power of neural networks. We used low-level EEG features as vectors for baseline and trained a model (no spatial information was taken into account), then transformed them into a multidimensional tensor (EEG as an image) and trained another model. Finally included temporal features (EEG as video) and trained the most sophisticated model. We counted on that CNNs are robust to inter- and intra-subject differences in data so created 2D and 3D CNNs along with dense neural networks. We also have taken spectral features of EEG data into account and created a new dataset where Fourier Transform has applied the data as a preprocessing step. We obtained our best accuracy with 3D CNNs; 85.46 for Dream Experience versus No Dream Experience and 55.07 for Dream Experience, Dream Experience Without Recall and No Dream Experience classification.

2 BACKGROUND

2.1 Dreams

A dream is an imaginary series of events that one experiences in his/her mind while he/she is asleep. Although not alike as two peas in a pod, dreaming brain continues working like an awake brain. Because of the similarities of a dreaming brain and an awake brain, dreams and dreaming are often associated with consciousness. [7] Level of consciousness varies according to sleep stages so does the dream experience. For normal human adults, sleep can be separated into two behaviourally different stages which are called REM and NREM sleep. The succession of NREM sleep stages followed by an episode of REM sleep is called a sleep cycle, and last 90 to 110 minutes. [8]

NREM sleep shows physiologically different patterns in EEG readings. According to patterns of brain signals collected by EEG and activities in the body, NREM sleep is divided into 3 distinguishable stages so-called N1, N2 and N3. In N1 stage, loss of alpha activity and the appearance of a low voltage mixed-frequency EEG are observable. Eye movements become slow and rolling, muscle tone relaxes, sense of falling and dream-like imagery occur. In N2 stage, the appearance of K complexes and sleep spindles are observable in EEG signals. Eye movements and muscle tone reduces more. Behaviourally, this stage qualifies fully as sleep because of disconnectedness from environment and increase in arousal threshold. In the N3 stage, EEG shows prominent slow waves in the delta range. Eye movements cease and muscle activity decreases further. Stage N3 is also referred to as slow-wave sleep, delta sleep or deep sleep. The threshold for arousal is higher than N2. REM sleep is also referred to as paradoxical sleep because of the similarity between EEG during REM sleep with EEG of waking or of stage N1. It is characterized by low-voltage fast activity EEG pattern. [8]

Dreaming experiences are often correlated with REM (rapid-eye-movement) sleep but it was shown that dreaming also occurs in NREM (non-REM) sleep. [7, 8] Regardless of sleep stages, however, analysis of the EEG recordings revealed that dreaming was linked to a drop in low-frequency activity in a region at the back of the brain called *posterior cortical hot zone*, a region that includes visual areas as well as areas involved in sensory integration. Changes in high-frequency activity in the brain also have effects such that increase in such activity in the *hot zone* during non-REM sleep is linked to dreaming. It was also found that an increase in high-frequency activity towards the front of the brain appears to be important in remembering what a dream was about, which is recalling the dream content. A similar pattern of activity is pertinent to the hot zone and beyond for dreams during REM sleep. In conclusion, dreaming is rooted in the spatial and temporal pattern of signals in particular regions of the brain regardless of the type of sleep. [7]

2.2 EEG Analysis

Electroencephalography (EEG) is an electrophysiological monitoring method to record the electrical activity of the brain. EEG measures voltage fluctuations resulting from action potentials fired from neurons. In clinical contexts, EEG refers to the recording of the brain's spontaneous electrical activity over a period of time, as recorded from multiple electrodes placed on the scalp. EEG recording is used ubiquitously to focus either on event-related

Band	Frequency (Hz)	Location
Delta	< 4	Frontally in adults, posteriorly in children; high-amplitude waves
Theta	4–7	Found in locations not related to task at hand
Alpha	8–15	Posterior regions of head, both sides, higher in amplitude on dominant side. Central sites (c3-c4) at rest
Beta	16–31	Both sides, symmetrical distribution, most evident frontally low-amplitude waves
Gamma	> 32	Somatosensory cortex
Mu	8–12	Sensory-motor cortex

Figure 1: Brain Waves [9]

potentials such as button press after stimulus or to analyze the type of neural oscillations (brain waves) observed for a period of time.

EEG has a poor spatial resolution. It is most sensitive to a particular set of post-synaptic potentials: those generated in superficial layers of the cortex, and non-sensitive to those who are located deeper in the brain. The electric potential generated by an individual neuron is far too small to be picked up by EEG, therefore, it always reflects the summation of the synchronous activity of thousands or millions of neurons that have similar spatial orientation. Although EEG has limited spatial resolution, it continues to be a valuable tool for research and diagnosis because of mobility, low cost and high temporal resolution (millisecond range). Scalp EEG recordings show oscillations at a variety of frequencies. Several of these oscillations have characteristic frequency ranges, spatial distributions and are associated with different states of brain functioning (e.g., waking and the various sleep stages). [9]

For our dataset, high-density EEG was used as opposed to standard EEG which greatly increased the spatial resolution such that source localization was doable.

Common Steps of EEG Data Analysis

The first step of EEG analysis is preprocessing raw EEG data. This data is usually not clean because of biological artefacts such as eye movements, muscle movements, cardiac effect or glossokinetic artefacts or environmental artefacts such as body movements, poor grounding or signal noise. Those artefacts can be removed by application of filters: a high-pass filter to remove the DC components of the signals and low pass filter to remove the high-frequency components. In EEG, frequencies above 90 Hz is rarely studied. Once the signals are clean, it is quite common to cut them in epochs of a few seconds and then extract features out of each one of these. The second step is feature extraction. EEG signals are complex, which makes them very hard to extract information with the naked eye. There are several techniques to take advantage of various characteristic features of EEG signals such as time domain features (mean, standard deviation, entropy etc.), frequency domain features (Fourier transform, wavelets etc.) and finally synchronicity features, which looks to the relationship between 2 or more EEG channels (coherence, correlation, mutual information etc.). There are other feature extraction methods such as EEG tomography, that allows us to compute the regions inside the brain that are active (applying the so-called inverse-problem approach). The next step, called feature selection, is optional and is used in the case in which there are a large number of features and only the ones that are more relevant to the study. In that case, one can apply statistical methods such as principal component analysis (PCA) or more complex techniques such as genetic algorithms. At last, using machine learning techniques, one can train a classifier to identify classes from features. [10]

2.3 Neural Networks

Neural networks are popular machine learning technique inspired by biological neurons. They are indeed mathematical functions which are particularly powerful on recognizing patterns in seemingly unrelated data. Recently, with the rapid increase in processing power, their popularity and diversity increased. Depending on the data type, problem schema and aim, network models run the gamut from densely connected networks to convolutional models, recurrent models and mixture of them.

An Artificial Neural Network is a collection of connected units or nodes called neurons. Each connection can transmit a signal from one neuron to another. An artificial neuron that receives a signal, processes it and then signals to other neurons connected to it. The signal at a connection between

neurons is a real number, and the output of each neuron is computed by some non-linear function of the sum of its inputs. Connections are called edges and typically, neurons are grouped in layers. Neurons and edges have weight to calculate outputs. The learning process is to find weights on edges which maps input to output the best. [11]

Convolutional Neural Networks are a variation of ANNs designed to require minimal preprocessing and particularly handful in image recognition tasks. CNNs were inspired by connectivity pattern between neurons of the animal visual cortex. Individual cortical neurons respond to stimuli only in a restricted region of the visual field known as the receptive field. The receptive fields of different neurons partially overlap such that they cover the entire visual field. CNNs work in a similar manner on images. Neurons in different layers process different regions on the image. The major advantage of CNNs is less need for hand-engineered feature selection for classification. [12]

3 DATA UNDERSTANDING

Dataset was collected by Sleep Laboratory at CHUV Hospital in Lausanne, Switzerland. It contains EEG recordings of 15 healthy subjects who spent 2 nights at the hospital (1 of the subjects spent only 1 night). In this dataset subjects only wore the cap. For sleep stage scoring purposes, four of the 257 electrodes placed at the outer canthi of the eyes were used to monitor eye movements (electrooculography, EOG), while electrodes located in the chin-cheek region were used to evaluate muscular activity (electromyography, EMG). However, EOG and EMG recordings were excluded from this project. Each subject was awakened from their sleep in random time intervals regardless of the REM phase or NREM phase of their sleep. [13, 7]

Subjects were awakened by a ring of an alarm. Immediately after awenkenings while eyes closed, they were asked if they were dreaming or not just before they heard the alarm. If the answer was yes, they were asked if they could recall what they have been dreaming of and if they could describe it. According to responses labels were given as **NE:** No Dream Experience, **DEWR:** Dream Experience without Recall of the Content and **DE:** Dream Experience with Recall of the Content. In our dataset responses were as below.

	Train			Validation			Test		
	NE	DEWR	DE	NE	DEWR	DE	NE	DEWR	DE
Single Channel Image	105k	120k	160k	4k	6k	4k	6k	26k	28k
Multichannel Image	12.5k	15k	15.5k	200	700	700	1k	3k	3.5k
Single Channel Video	1k	1k	1.6k	30	50	50	50	250	300
Multichannel Video	1k	1k	1.6k	20	60	60	80	250	300
Raw	100k	125k	150k	2k	4k	8k	6k	18k	36k
FFT	12k	15k	15k	200	500	1k	1k	3k	3.5k

Figure 2: Data Distributions After Balancing and Sampling (20%)

Stage N2:
13.99 % NE
46.75 % DEWR
40.26 % DE
Stage N3:
20.31 % NE
34.38 % DEWR
45.31 % DE
Stage REM:
13.48 % NE
24.72 % DEWR
61.80 % DE

Full night EEG recordings for each subject were delivered. For each subject and for each night data files were provided as matrix shape. Every single file is a recording from the beginning of sleep until the subject awakened again. Each row represents each time step, therefore, the number of rows has varied length whereas columns represent each electrode, therefore, a fixed length of 257.

Datasets were received with two formats, uploaded directly to MLO clusters and stored under */mlodata1/yuecetue/dream* directory as *dream_data* and *dream_data_fft_SW*. Files under *dream_data* are referred as raw data whereas files under *dream_data_fft_SW* are those obtained after Fourier Transform. Each subdirectory started with H0** belongs a subject and each file in these subdirectories belongs to a trial. Naming convention (e.g file) *H009_E1_NREM*

_S01.mat belongs to subject H009, night 1, awakened from NREM stage and the first awakening for that night respectively. Labels were fetched from *Dream_reports_healthy.xlsx* file and channel coordinates were extracted to *channelcoords.mat* file as 257x3 matrix format X, Y, Z coordinates of each electrode respectively.

4 DATA PREPARATION

4.1 Prepocessing & Spectral Analysis

As default pre-processing step recordings were cleaned from artefacts and noises with standard Butterworth filter. Segment excluded recordings denote partially corrupted data, were not included. Files were received after initial preprocessing step with the format as described above. As a result of the discussions, only the last 20 seconds before the awakenings were decided to be of interest because brain signals of on this time are found the most correlated ones with dreaming experience. [7]

Fourier transform was applied to last 2 minutes of recordings for 2 seconds of window size with 0.5-second sliding. Two bandpass filter of range 1-4 Hz (Delta) and 20-50 Hz (Beta-Gamma) were applied because of the correlations of low and high-frequency activity with dream experience as mentioned above. Reason to choose window size as 2 second was to be able to catch the slow waves (1-4 Hz). Sum of the square of complex amplitude (power) value was calculated for each electrode separately. These power values were then used instead of raw values.

Both raw data and FFT data (referred to data after applied Fourier Transform) was read by *prepare_data.py* script. The number of columns of FFT data was doubled: first delta power band values then beta-gamma band values were stacked side by side. Those versions were stored in the same location as *20sec_raw_data_zip.npz* and *2sec_fft_data_zip.npz* In both formats, 372 trial files (recording single awakening) were provided, 371 of them were used. Train and test datasets were separated by trial not by subject because each label came from a single trial. Dataset was split to 90% train and to 10% test. 20% of the test set was used as a validation set. Because of unbalanced distribution of labels; roughly 50% of labels belonged DE, 35% of belonged to DEWR and 15% of belonged to NE, train set was balanced by selective subsampling. No subsampling applied for the test set.

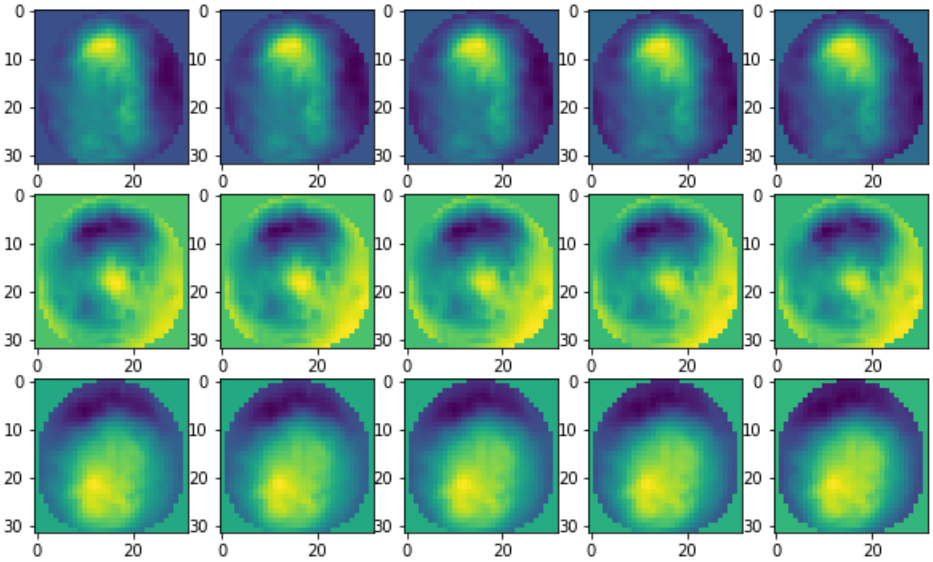

Figure 3: EEG As Image - 0.5 Second Time Difference Between Rows *from H009_E1_NREM _S01.mat*

4.2 EEG Signal To Image & Video

We treated the EEG classification problem with EEG as image and EEG as video approaches. For each time step, the values of 256 electrodes were used to generate an image. Value of reference electrode (column 257) was excluded for all since it was always value 0. To get the correct values for each electrode, the average of raw values of 256 electrodes subtracted from each of the electrodes for each time step (each row). This step was only performed for raw data not for FFT data. For both data normalization through time per channel were applied such that mean of a channel for full recording was subtracted and values divided to the standard deviation of that channel for recording time.

To create EEG images, the first step was to project the location of electrodes into 2-dimensional space. While creating the images, spatial distributions and relative distances of electrodes to each other were important because: first, it might be the case that activity or inactivity in some part of the brain might account for dreaming experience or recalling of dreaming experience eg. and we would like to catch this activity with the shapes created

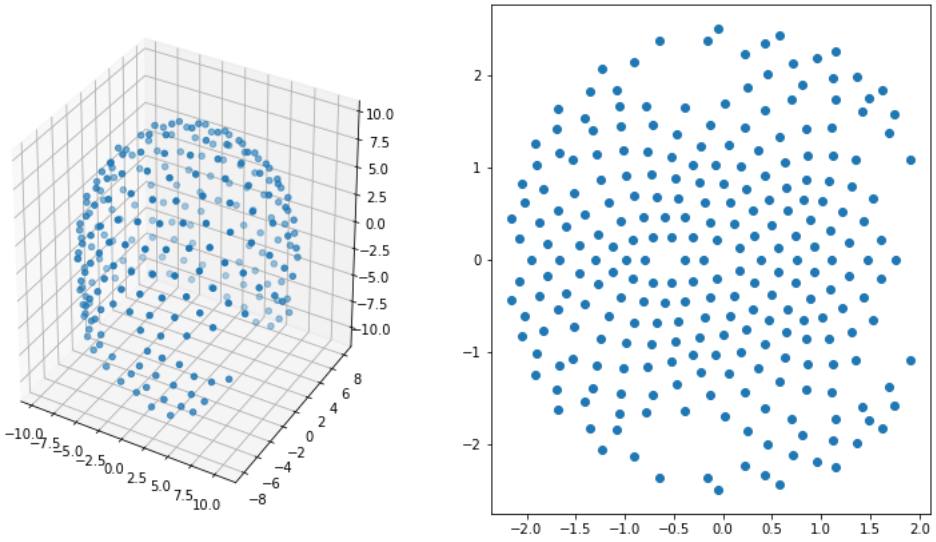

Figure 4: Real Locations of Electrodes 3D - AEP Locations 2D

by values of electrodes positioned this part of the head. Second, the values of electrodes which are close to each other tend to have similar values because of the working principle of EEG. With these concern, we decided to use the Azimuthal Equidistant Projection algorithm (AEP) to project locations of electrodes to 2-dimensional space.

We created 32x32 image for each time step of recording of raw data. We used values of 256 electrodes for each time step, empty pixels were filled with standard cubic interpolation, the single colour channel was used. Images then normalized, no noise was added. Images of FFT data were created with the same methodology but with 2 colour channels. In these multichannel images, power values of delta and beta-gamma frequency bands were replaced with raw data values. Similarly, cubic interpolation and normalization were applied but among the same channels.

Videos were created from consecutive EEG images. For raw data, videos were created 100 frames with 10 frame slide, which is equal to 0.2 seconds of recordings. For FFT data, videos were created 10 frames with 1 frame slide, which is equal to 20 seconds of recording. Both videos and images, labels were given as the same as the label of the trial.

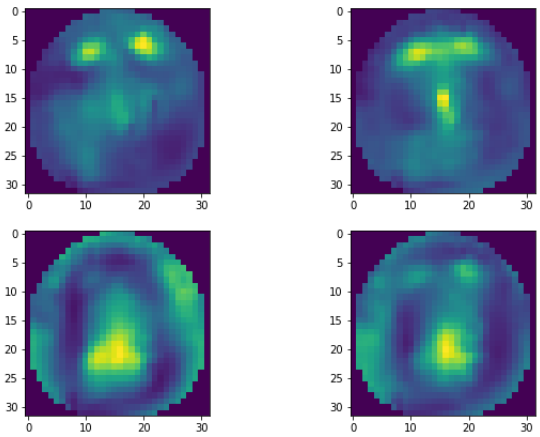

Figure 5: EEG As Image - 20 Seconds Between Rows First Column Delta, Second Column Beta-Gamma Band
from H009_E1_NREM_S01_DeltaGamma.mat

5 MODELS

For this project, multiple neural network models were implemented to find patterns in EEG data and to classify recordings. Three approaches were considered. All models were implemented by using Keras library with Tensorflow backend as Sequential Models because of simplicity and possibility fast development. Hyper-parameter tuning was performed via a grid search. For all models, **activation functions ReLu, Sigmoid, Tanh and None**; dropout rate **dropout rate .5, 0.3**; **kernel size 3,5,7**; **number of neurons in last fully connected layer 128,256,512** and **L1 and L2 regularizer with lambda 0.0001** were tested. Architectures were decided with combinations of hyper-parameters which gave the best result.

5.1 Baseline Neural Network

Simplest approach was to treat recordings of each electrode as time series data. In this approach, we treated recordings of 256 electrodes of each time step as a data point. We ignored both spatial and temporal information. This model was built as a dense neural network and trained it as a baseline model in order to understand necessity and sufficiency of temporal and spatial information embedded in EEG.

Model	Number of Paramaters
Baseline NN - Single	43k
Baseline NN - Multi	76k
CNN - Image - Single	730k
CNN - Image - Multi	450k
CNN - Video - Single	2.5M
CNN - Video - Multi	1.9M

Table 1: Model Summaries

Baseline neural network consisted of four dense layers, one drop-out layer and last softmax layer with three classes. Number of filters in dense layers were 128, 64, 32 and 16 respectively. Kernel initializer was chosen from gloroth uniform distribution as common practice. To prevent overfitting, L2 kernel regularizer was used with parameter 0.0001 and drop-out rate was chosen as 0.5. Sigmoid activation function was chosen for the first layer to scale both positive and negative raw values, ReLu activation was used for the rest of the layers.

5.2 CNN for EEG Image

The second approach was EEG as an image. We aimed to take advantage of the power of Convolutional Neural Network by turning EEG data into images. In this approach, we created an image from recordings of 256 electrodes in each time step. These images represent a snapshot of a sleeping brain in a time step. Images were created as previously described.

We built a VGG style CNN with four, two and one 2D convolutional layers; the number of filters was chosen 32, 64 and 128 respectively. Kernel size was chosen as 5 for single channel images and as 3 for multichannel images, kernel initializer was gloroth uniform and same padding was used for all convolutional layers. Convolutional layers were separated by a max-pool layer with pool size 2 and valid padding applied without strides specified. To prevent overfitting, L2 kernel regularizer with parameter 0.0001 was added.

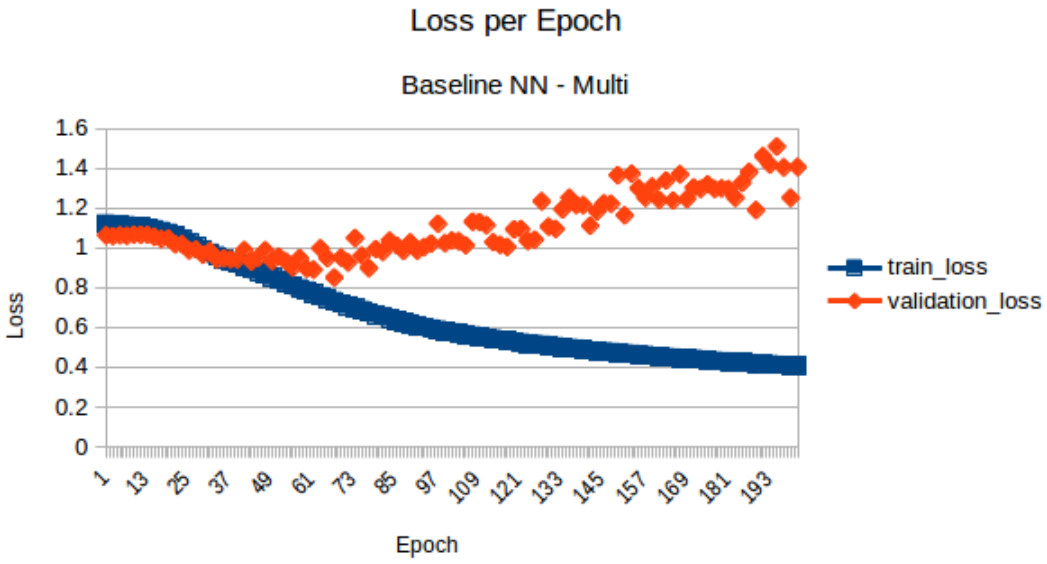

Figure 6: Baseline Training

Finally, a fully connected layer with 256 nodes, drop-out layer with rate 0.5 and softmax layer were added.

5.3 CNN for EEG Video

The third approach was EEG as video. Dreaming, as far as we know, is an activity that intrinsically time-dependent. For this approach, we built CNN-Video for EEG videos where each video consists of a batch of EEG images to preserve time information in dreaming phase. Here 3D version convolution layers and filters were used.

Architecture for 3D CNNs was similar with 2D CNN but one layer less. The structure was 4 and 2 convolutional layers with 32 and 64 filters then fully connected layer and drop-out layer with rate 0.5. The number of nodes in the fully connected layer was decided 256 for single-channel videos and 128 for multichannel videos. Convolution was performed on x, y and time dimension, with kernel size 3x3x2 for multichannel and 5x5x10 for the single channel was set. No activation function was specified for single-channel videos whereas sigmoid was set for the multichannel model. The dropout rate was set to 0.5 and L2 regularizer with weight 0.0001 was used.

Model	**Data**	**Training Accuracy %**	**Validation Accuracy %**	**Test Accuracy %**
Baseline NN	Raw EEG	64.93	58.45	54.95
Baseline NN	FFT EEG	40.10	57.14	48.39
CNN - Image	Multichannel Image	42.13	43.04	50.13
CNN - Image	Single Channel Image	64.50	47.69	45.17
CNN - Video	Multichannel Video	72.69	45.58	55.07
CNN - Video	Single Channel Video	63.89	38.92	43.44

Table 2: Results Summary For 3 Classes: DE - DEWR - NE

The reason of one less layer was to simplify the models. Since we created the videos from batches of images we reduced the number of sample to one percent for raw data (each video consists of a batch of 100 images)and one-tenth for FFT data (batch of 10 images). Therefore, we reduced the number of parameters of the model to be optimized in order to get better results.

6 RESULTS

Each network was trained with its own data format and data samples. The number of data used and distribution of the labels are provided in Figure 2. Models were trained for three classes and two classes. In two class case, only DEWR data were excluded; Dream Experience(DE) vs No Dream Experience (NE) data were fed with the same label distribution. For single channel models, datasets were randomly subsampled with 0.2 of their size for training, validation and test data in order to obtain the results faster. Please note that early stopping condition was applied when validation loss started to increase.

Baseline

Baseline models were trained for both two and three classes for 30 epochs, batch size 100 and 10 for raw and FFT data respectively. Stochastic gradient descent optimizer was used with learning rate 0.0005, decay 1e-6 and momentum 0.9. For raw data, baseline model showed a tendency to decrease in loss and increase in accuracy for both training and validation set. However, for the FFT data baseline model showed no improvement. It fitted the data in the first epoch and no changed observed afterwards. Therefore, it is highly likely this result reflects just the trivial accuracy for the dataset for both 2-class and 3 class classification.

CNN for EEG Image

CNN-Image models were trained for both two and three classes for 30 epochs, batch size 100 and 10 for raw and FFT data respectively. Stochastic gradient descent optimizer was used with learning rate 0.0005, decay 1e-6 and momentum 0.9. For 2-class classification, this model showed an increase in training accuracy and validation accuracy up to some point while the number of epochs increased. For 3-class classification, the model displayed large fluctuations in loss and accuracy. After 5 epochs, validation loss started to increase. Therefore, results reported here belong the models stopped training just before validation loss started to increase again. (Various number of epochs)

CNN for EEG Video

CNN-Video models were trained for both two and three classes for 30 epochs, batch size 32 and 10 for raw and FFT data respectively. Stochastic gradient descent optimizer was used with learning rate 0.0005, decay 1e-6 and momentum 0.9. For two-class classification, loss tended to decrease while the number of epochs increased as usual for both data type however, accuracy fluctuated largely for 3-class classification of raw data. This might stem from sampling. Since training time was too long (more than 7 hours for 0.2 downsampling for 30 epochs) downsampling was necessary but results are not fairly well.

Model	**Data**	**Training Accuracy %**	**Validation Accuracy %**	**Test Accuracy %**
Baseline NN	Raw EEG	88.88	85.95	80.33
Baseline NN	FFT EEG	59.23	80.0	78.95
CNN - Image	Multichannel Image	95.31	77.0	80.04
CNN - Image	Single Channel Image	94.11	72.60	82.23
CNN - Video	Multichannel Video	87.28	72.62	85.46
CNN - Video	Single Channel Video	92.08	84.70	80.04

Table 3: Results Summary For 2 Classes: DE - NE

7 CONCLUSION & FUTURE WORK

This work was motivated by a deep interest to the human brain and consciousness. Neuroimaging techniques are keys for the mechanistic understanding of the human brain and EEG is one of the cheapest and a highly accessible way to examine it, Unfortunately, it is too complicated to interpret simply with naked-eyes but luckily, neural networks came to rescue. They proved their adequacy for performing many tasks; sometimes better than humans. Why not can they be helpful in discovering brand new brain functionalities?

Here, we proposed multiple methodologies for representation learning and classification of EEG time series. We adopted EEG as image and EEG as video approaches. It turned out that there exist dreaming patterns in EEG recordings of sleeping brain which can be detected by neural networks. However, these patterns are embedded more in temporal features than spatial features since 3D CNNs which took temporal information into account outperformed 2D CNNs. Another implication may be that neural networks can perform equally good without any pre-processing step, namely Fourier Transform. However, it is important to remember, our Fourier Transform took in a very long period of duration (2 minutes) where sleep stage can physiologically and behaviourally differ from the beginning to end of the recording. Therefore, we might have introduced redundant and erroneous information which confused the networks.

For future work, given that these kinds of data (no as observable pattern as cognitive load classification tasks) is new in EEG classification area, it had better experiment with well developed neural networks like EEGLab[6], Braindecode[4] and EEGNet[14] where both spatial and temporal characteristic of EEGs were considered. Since all use Fourier Transformed version of EEG data, the first step is to create new datasets where Fourier Transform is applied in a more reasonable period and with more reasonable sliding size. Another direction may be a visualization of the networks, which possibly gives insight into how well the networks discover and identify specific regions in the brain.

8 APPENDIX

Please note that all code files, scripts for data preparation and model testing are in https://github.com/effervescent-shot/Dream-Prediction. All necessary information: file structures, comments and explanations for how to run a model are included. Architectures can be found in result files. Sample results are provided under Results directory on GitHub.

References

[1] A. Krizhevsky, I. Sutskever, and G. E. Hinton, "Imagenet classification with deep convolutional neural networks," in *Advances in neural information processing systems*, pp. 1097–1105, 2012.

[2] A. Karpathy, G. Toderici, S. Shetty, T. Leung, R. Sukthankar, and L. Fei-Fei, "Large-scale video classification with convolutional neural networks," in *Proceedings of the IEEE conference on Computer Vision and Pattern Recognition*, pp. 1725–1732, 2014.

[3] K. K. Ang, Z. Y. Chin, H. Zhang, and C. Guan, "Filter bank common spatial pattern (fbcsp) in brain-computer interface," in *Neural Networks, 2008. IJCNN 2008.(IEEE World Congress on Computational Intelligence). IEEE International Joint Conference on*, pp. 2390–2397, IEEE, 2008.

[4] R. T. Schirrmeister, J. T. Springenberg, L. D. J. Fiederer, M. Glasstetter, K. Eggensperger, M. Tangermann, F. Hutter, W. Burgard, and T. Ball, "Deep learning with convolutional neural networks for eeg decoding and visualization," *Human brain mapping*, vol. 38, no. 11, pp. 5391–5420, 2017.

[5] C. Tan, F. Sun, W. Zhang, J. Chen, and C. Liu, "Multimodal classification with deep convolutional-recurrent neural networks for electroencephalography," in *International Conference on Neural Information Processing*, pp. 767–776, Springer, 2017.

[6] P. Bashivan, I. Rish, M. Yeasin, and N. Codella, "Learning representations from eeg with deep recurrent-convolutional neural networks," *arXiv preprint arXiv:1511.06448*, 2015.

[7] F. Siclari, B. Baird, L. Perogamvros, G. Bernardi, J. J. LaRocque, B. Riedner, M. Boly, B. R. Postle, and G. Tononi, "The neural correlates of dreaming," *Nature neuroscience*, vol. 20, no. 6, p. 872, 2017.

[8] G. T. Francesca Siclari, *Sleep and Dreaming*. Academic Press, 2016.

[9] "Electroencephalography." https://en.wikipedia.org/wiki/Electroencephalography. [Online; accessed 20-October-2018].

[10] "Eeg signal processing." https://www.neuroelectrics.com/blog/eeg-signal-processing-for-dummies/. [Online; accessed 20-October-2018].

[11] "Artificial neural network." https://en.wikipedia.org/wiki/Artificia_neural_network/. [Online; accessed 25-December-2018].

[12] "Convolutiona neural network." https://en.wikipedia.org/wiki/ Convolutional_neural_network. [Online; accessed 25-December-2018].

[13] C. Iber, S. Ancoli-Israel, A. Chesson, and S. Quan, "Westchester, il: American academy of sleep medicine; 2007," *The AASM manual for the scoring of sleep and associated events: rules, terminology and technical specifications*, vol. 4849, 2007.

[14] V. J. Lawhern, A. J. Solon, N. R. Waytowich, S. M. Gordon, C. P. Hung, and B. J. Lance, "Eegnet: A compact convolutional network for eeg-based brain-computer interfaces," *arXiv preprint arXiv:1611.08024*, 2016.